EFFECT OF BROMINE SUBSTITUTION ON THE LIFETIMES AND OZONE DEPLETION POTENTIALS OF ORGANIC COMPOUNDS

Robert E. Huie, Vladimir L. Orkin, Florent Louis, Sergey N. Kozlov, and Michael J. Kurylo

Physical and Chemical Properties Division,
National Institute of Standards and Technology
Gaithersburg, Maryland 20899-8381

301-975-2559 robert.huie@nist.gov
301-975-4418 vladimir.orkin@nist.gov
33-3-20-43-63-32 flouis@pop.univ-lille1.fr
7 (095) 939-7318 kozlov@chph.ras.ru
202-358-0237 mkurylo@mtpe.hq.nasa.gov

INTRODUCTION

Although the bromofluorocarbon compounds known as halons are excellent fire suppressants, their production is being phased out due to the considerable danger they pose to the Earth's ozone layer. A number of non-brominated substances have been proposed and tested, but the effort to find replacements continues to return to bromine due to the chemical characteristics of this element as a chemically active flame suppressant. Thus, a number of classes of bromine-containing molecules have been proposed for investigation as to their fire-suppression characteristics. Before candidate replacements can be placed into service, it is important to establish their environmental effects, particularly the projected ozone depletion potential. Generally, these replacement compounds are designed to be reactive toward atmospheric hydroxyl radicals. This reaction leads to chemical transformations that ultimately lead to the removal of the bromine from the atmosphere. Additionally, photolysis of these compounds in the atmosphere will release Br and may further shorten their lifetimes. In order to quantitatively evaluate the impact of these compounds in the atmosphere, we have investigated the reactivity of several classes of reactants toward OH, both experimentally and computationally. Rate constants were determined over the temperature range of at least 250 K to 370 K. In addition, we have measured the absorption spectra of most of these compounds down to 160 nm. We have then utilized this information to derive predicted ozone depletion potentials.

Experimental Section

UV Absorption Cross-Section Measurements. The absorption spectra of the brominated compounds to be analyzed were measured over the wavelength range of 160-280 nm using a single beam apparatus consisting of a 1 m vacuum monochromator equipped with a 600 lines/mm grating and a photomultiplier. The radiation source was a deuterium lamp. Spectra were recorded at increments of 0.5 nm at spectral slit widths of 0.5 nm. The pressure inside the (16.9 ± 0.05) cm absorption cell was measured by a manometer at T = (295 ± 1) K. Absorption spectra of the evacuated cell and of the cell filled with a gas sample were alternately recorded several times, and the absorption cross sections were calculated from the differences. The

complete spectra were constructed from data taken over several overlapping wavelength ranges. Data over each range were obtained at several pressures to verify adherence to the Beer-Lambert absorption law. The overall instrumental error associated with uncertainties in the path length, pressure, temperature stability, and the measured absorbance was estimated to be less than 2% over most of the wavelength range, increasing to ca. 10-20 % at the long-wavelength ends of the spectra. Mixtures containing 2%, 10%, and 100% of the compounds under study were used at pressures in the cell ranging from 4 Pa to 120 kPa (0.03 - 900 Torr).

OH Reaction Rate Constant Measurements. The principal component of the flash photolysis-resonance fluorescence (FPRF) apparatus is a Pyrex reactor (of approximately 50 cm^3 internal volume) thermostated with water or ethanol circulated through its outer jacket. Reactions were studied in argon carrier gas (99.9995% purity) at a total pressure of 13.33 kPa (100.0 Torr). Flows of dry argon, argon bubbled through water thermostated at 276 K, and reactant mixtures (containing 0.01%-0.1% of the reactant diluted with argon) were premixed and flowed through the reactor at a total flow rate between 0.6 and 1.4 $cm^3\ s^{-1}$, STP. The concentrations of the gases in the reactor were determined by measuring the mass flow rates and the total pressure with a manometer. Flow rates of argon, the H_2O/argon mixture, and reactant/inert gas mixtures were measured by calibrated mass flow meters. Hydroxyl radicals were produced by the pulsed photolysis (1-4 Hz repetition rate) of H_2O (introduced via the 276 K argon / H_2O bubbler) by a xenon flash lamp focused into the reactor. The radicals were then monitored by their resonance fluorescence near 308 nm, excited by a microwave-discharge resonance lamp (330 Pa or 2.5 Torr of a ca. 2% mixture of H_2O in UHP helium) focused into the reactor center. The resonance fluorescence signal was recorded on a computer-based multichannel scanner (channel width 100 μs) as a summation of 2,000-5,000 consecutive flashes. The radical decay signal at each reactant concentration was analyzed as described previously [1] to obtain the first-order decay rate coefficient due to the reaction under study.

Computational Determinations of OH Kinetics. Fully optimized geometries, harmonic frequencies, and zero-point energy corrections, ZPE, of reactants, transition structures and products were computed with the second-order Møller-Plesset perturbation theory, UMP2, using the 6-311G(2d,2p) basis set. Electron correlation was calculated with the fourth-order Møller-Plesset perturbation theory in the space of single, double, triple and quadruple excitations with full annihilation of spin contamination, [2] PMP4(SDTQ). These single-point energy calculations were carried out with the 6-311G(3df,2p) basis set using the geometries previously optimized at the MP2/6-311G(2d,2p) level. All relative energies quoted and discussed in this paper include zero-point energy corrections with unscaled frequencies obtained at the MP2/6-311G(2d,2p) level.

Rate constants, *k(T)*, were computed using the following transition state theory expression [3]:

$$k(T) = \Gamma(T) \times \frac{k_B T}{h} \times \frac{Q^{TS}(T)}{Q^{OH}(T) Q^{CHXYZ}(T)} \times \exp\left(-\frac{\Delta E}{k_B T}\right) \qquad (1)$$

Where: $Q^{OH}(T)$, $Q^{CHXYZ}(T)$, $Q^{TS}(T)$, are the total partition functions for the hydroxyl radical, halomethane of type CHXYZ, and transition state respectively at temperature T; ΔE is the activation energy including zero-point energy and thermal corrections to the internal energy; k_B is Boltzman's constant, and h is Planck's constant. For all species, the total partition function can be cast in terms of the translational, (Q^X_T), rotational, (Q^X_R), electronic, (Q^X_e), and

vibrational, (Q^X_v), partition functions. In computing the electronic partition function for the OH radical, Q^{OH}_e, the multiplicity of the states $^2\Pi_{3/2}$ and $^2\Pi_{1/2}$ and the energy gap of 139.7 cm^{-1} between the low-lying electronic states have been taken into consideration. As in our previous work, the tunneling correction *Γ(T)* in equation (1) is computed by the simple Wigner's formalism [4]:

$$\Gamma(T) = 1 + \frac{1}{24}\left(\frac{h\nu^{\neq}}{k_B T}\right)^2 \qquad (2)$$

Where $\nu^{\neq}$ is the imaginary frequency at the saddle point and the other terms have the same meaning as in equation (1). The rate constant calculations over the temperature range 250-400 K were carried out using the TURBO-RATE program. [5]

Results and Discussion

UV Absorption Spectra All of the bromine-containing compounds absorb ultraviolet radiation strongly in the 195 nm – 215 nm region, where photodissociation in the lower stratosphere is most important. This reduces their atmospheric lifetimes, but contributes to the ozone depletion potential. The measured absorption cross sections for this region are utilized in our calculations of the ozone depletion potentials for these species. The results of our measurements on bromine-containing compounds are shown in Figures 1 – 3, along with some other gasses for comparison.

Figure 1. UV absorption spectra of bromopropanes and 2-bromo-1,1-difluoroethyl methyl ether

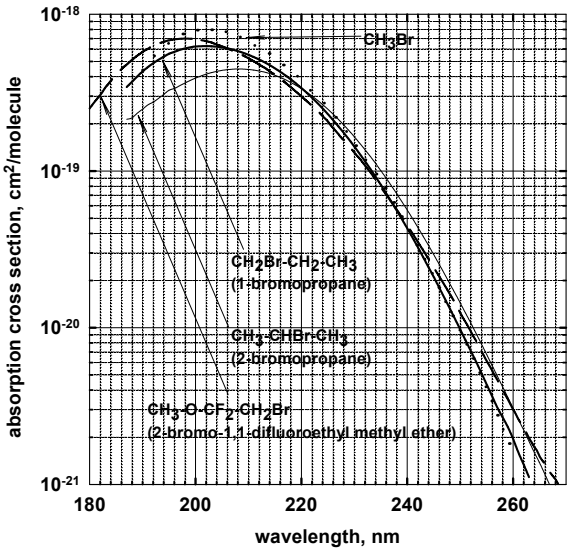

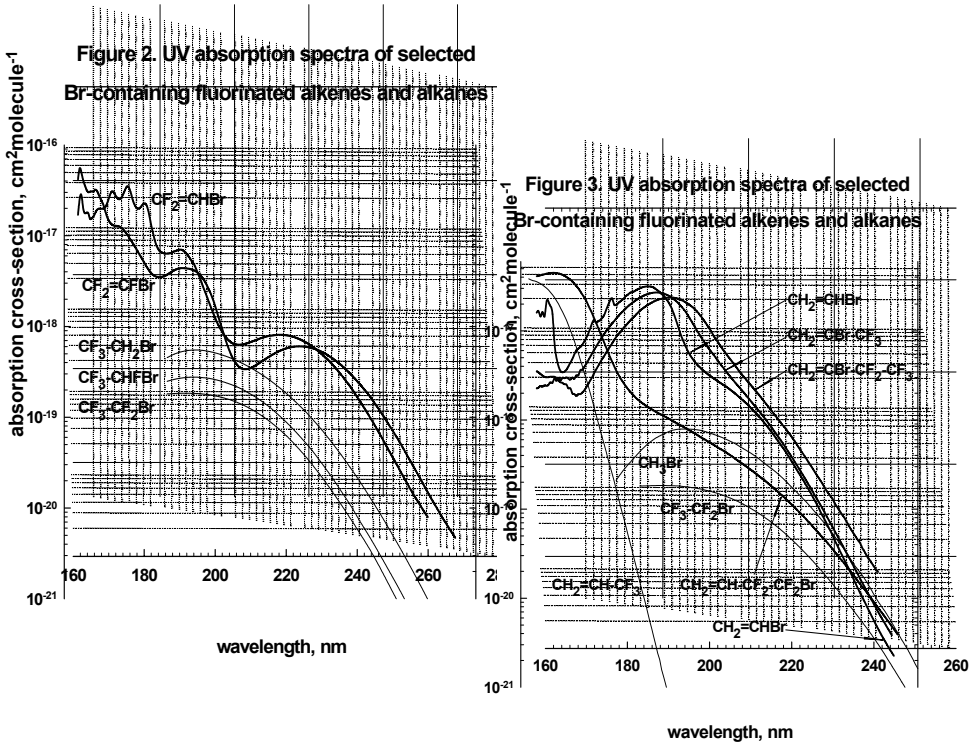

Experimental Kinetics: The results of our measurements on the reactions of hydroxyl radicals with five bromofluoro-alkenes at different temperatures are presented in Figure 4. The derived Arrhenius parameters for the reactions are listed in Table 1. The effect of halogenation on alkene reactivity is quite complicated. Nevertheless, one can speculate on the correlation between reactivity and structure of these halogenated alkenes. Fluorination of one olefinic carbon tends to deactivate while fluorination of the second olefinic carbons tends to compensate that deactivation. This suggests that the alkene reactivity toward OH depends mainly on the geometrical localization of π-electron density. Bromination of the olefinic carbon increases the reactivity of fluorinated alkenes while Br on a remote carbon has essentially no effect (Figure 5).

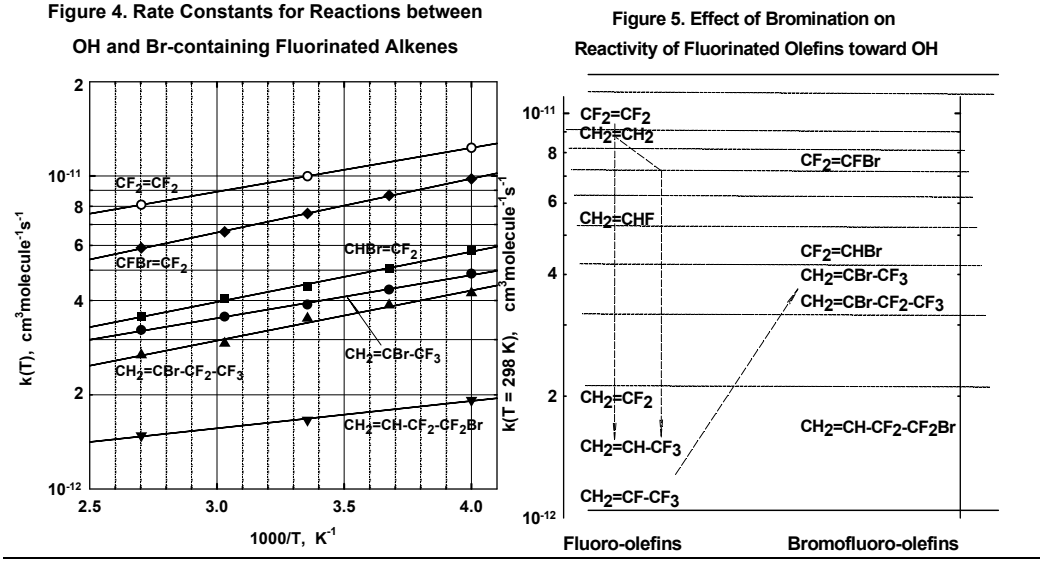

Arrhenius Parameters for OH Reactions of Br-containing Fluoroalkenes and their Estimated Environmental Parameters

Molecule	$A\times10^{12}$, $cm^3molecule^{-1}s^{-1}$	$E/R \pm \Delta E/R$, K	$k(298)\times10^{12}$ $cm^3molecule^{-1}s^{-1}$	Atmospheric lifetime, days	ODP
$CF_2=CF_2$	3.39 ± 0.22	–323 ± 11	9.98± 0.02	*1.1*	
$CFBr=CF_2$	2.02 ± 0.12	–396 ± 18	7.62 ± 0.06	*1.4*	*0.0022*
$CHBr=CF_2$	$1.30^{+0.22}_{-0.18}$	–370 ± 47	4.53 ± 0.10	*2.4*	*0.0015*
$CH_2=CBr-CF_3$	$1.36^{+0.17}_{-0.14}$	–317 ± 34	3.94 ± 0.06	*2.4*	*0.0034*
$CH_2=CBr-CF_2-CF_3$	$0.98^{+0.35}_{-0.26}$	–369 ± 90	3.39 ± 0.14	*3.1*	*0.0030*
$CH_2=CH-CF_2-CF_2Br$	$0.85^{+0.15}_{-0.12}$	–201 ± 46	1.68 ± 0.05	*6.7*	*0.0043*

Atmospheric lifetimes and ODPs were estimated in the manner typically used for long-lived compounds. Such estimations assume a uniform tropospheric distribution that is not correct for short-lived compounds. ODPs were estimated using the calculated lifetime of CF_3Br equals to 65 years and its ODP(CF3Br) = 13. [6]

Figure 6. Rate Constants for Reactions of OH with 1-bromopropane, 2-bromopropane, and propane

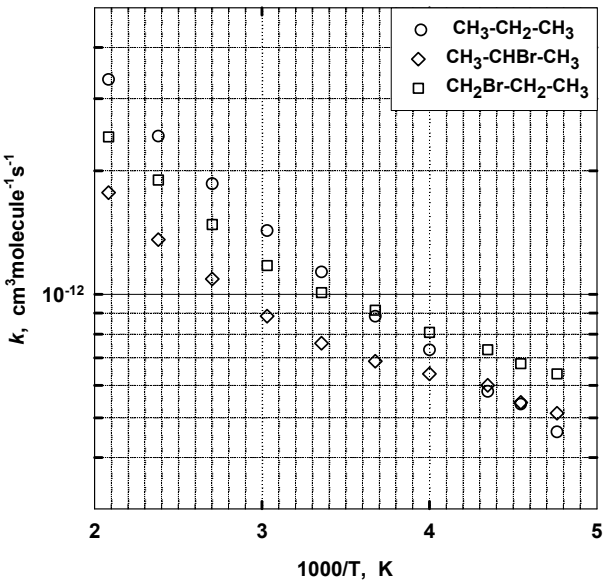

The reactivity of OH toward both 1- and 2-bromopropane has been determined over the temperature range 210 K to 480 K. The Arrhenius plots presented in Figure 6 show curvature due to the different rate constants for abstraction from the different types of C-H bonds in the molecules. In Table 2, we present the Arrhenius parameters for the temperature range below 298 K.

Table 2. Arrhenius Parameters for OH Reactions of propane and bromopropanes

Molecule	$A\times10^{12}$, $cm^3molecule^{-1}s^{-1}$	E/R, K	$k(298)\times10^{12}$ $cm^3molecule^{-1}s^{-1}$	Atmospheric lifetime, days	ODP
$CH_3CH_2CH_2Br$	3.04	329	1.01	*14*	*0.015*
$CH_3CHBrCH_3$	1.90	275	0.76	*19*	*0.018*

Figure 7. The Rate Constants for the Reaction between OH and 2-bromo-1,1-difluoroethyl methyl ether

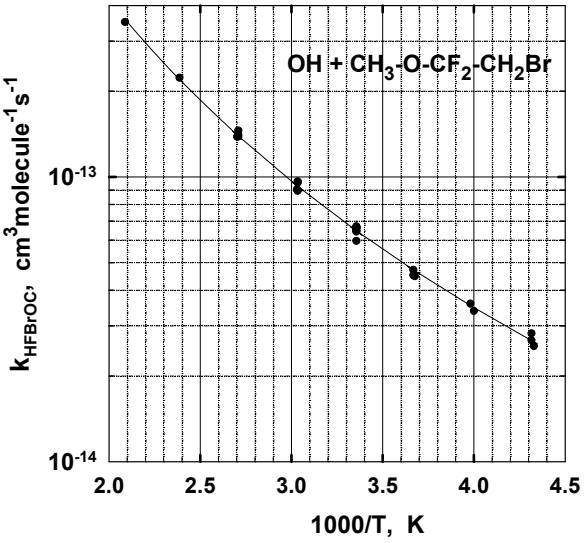

In Figure 7 we present our results on the kinetics of the reaction of OH with the bromine-substituted fluoroether $CH_3OCF_2CH_2Br$. The Arrhenius plot is clearly curved, which we ascribe to abstraction at the two different C-H sites. The results can be represented by the expression $k = 5.24 \times 10^{-14}(T/298)^{3.77}\exp(+(63\pm202)/T)$ cm^3 $molec^{-1}$ s^{-1}.

Computational Kinetics: The computational screening approach was applied to a series of halogenated methanes for which reliable kinetic data were available. [7] By this means, we were able to demonstrate that the chosen level of theory could provide calculated rate constants that were within better than factors of three of the experimental values, and typically within better that a factor of two. The results of these calculations are presented in Table 3 for the bromine-containing methanes. [8]

Table 3. Calculated Arrhenius Parameters for Reactions with OH at the PMP4(STDQ)/6-311G(3df,2p) Level of Theory, Estimated Atmospheric Lifetimes, and ODPs

Molecule	$A\times10^{12}$, $cm^3molecule^{-1}s^{-1}$	E/R K	$k(298)\times10^{14}$ $cm^3molecule^{-1}s^{-1}$	Atmospheric lifetime, years	ODP
CH_3Br	5.4	1610	2.4	*2.5*	*1.2*
CHF_2Br	1.5	1550	1.0	*6.0*	*1.6*
CH_2FBr	3.8	1440	3.0	*1.9*	*0.59*
CH_2ClBr	2.2	945	9.2	*0.52*	*0.23*
CHFClBr	2.2	920	6.8	*0.70*	*0.27*
CH_2Br_2	2.5	995	8.9	*0.55*	*043*
$CHFBr_2$	1.6	825	10.0	*0.46*	*0.30*
$CHCl_2Br$	0.8	330	26.4	*0.15*	*0.047*
$CHClBr_2$	0.8	250	34.6	*0.11*	*0.08*

An interesting observation is that whereas more heavily substituted methanes have lower pre-exponential factors, this is more than made up in their lower values of E/R. Thus, the predicted lifetimes decrease from 2.5 years for CH_3Br to 0.11 years for $CHClBr_2$, with the calculated ODP values decreasing from 1.2 to 0.08. In our comparison between experimental and computational results, we found that the rate constants for the faster reactions seemed to be somewhat overestimated. Thus, we would expect that the actual rate constants for the faster reactions ($k_{298} > 10^{-13}$ cm^3 $molec^{-1}$ s^{-1}) to be somewhat lower and the lifetimes and ODPs larger.

Fate of the Bromine: General mechanisms for atmospheric degradation of fluorinated Br containing alkenes has been developed based on the analysis of available kinetic data. When bromine is substituted on an olefinic carbon, the scheme below suggests that it is ejected early in the reaction.

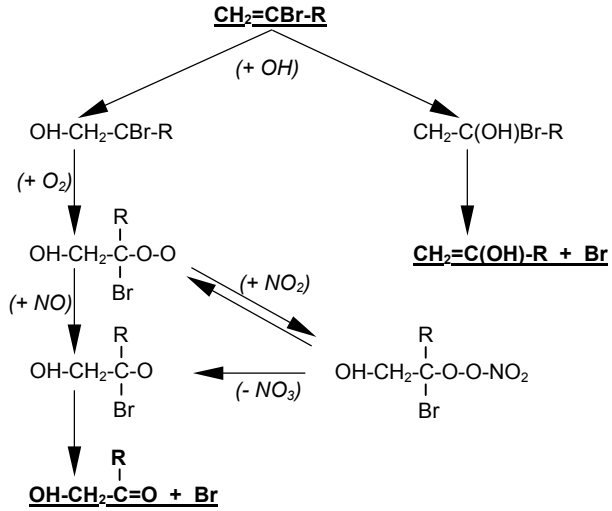

When bromine resides on a carbon removed from the double bond, the mechanism is somewhat more complex, as illustrated below for decomposition of CH_2=CH-CF_2-CF_2Br:

OH + CH_2=CH-CF_2-CF_2Br (+ M)	→	$HOCH_2$-CH-CF_2-CF_2Br (+M)
$HOCH_2$-CH-CF_2-CF_2Br + O_2	→	$HOCH_2$-CH(O_2)-CF_2-CF_2Br
$HOCH_2$-CH(O_2)-CF_2-CF_2Br + NO	→	$HOCH_2$-CHO-CF_2-CF_2Br + NO_2
$HOCH_2$-CHO-CF_2-CF_2Br	→	CH_2OH + O=CH-CF_2-CF_2Br
CH_2OH + O_2	→	O=CH_2 + HO_2
	Or	
OH + CH_2=CH-CF_2-CF_2Br (+ M)	→	CH_2-CH(OH)-CF_2-CF_2Br (+M)
CH_2-CH(OH)-CF_2-CF_2Br + O_2	→	$C(O_2)H_2$-CH(OH)-CF_2-CF_2Br
$C(O_2)H_2$-CH(OH)-CF_2-CF_2Br + NO	→	COH_2-CH(OH)-CF_2-CF_2Br + NO_2
COH_2-CH(OH)-CF_2-CF_2Br	→	O=CH_2 + CH(OH)-CF_2-CF_2Br
CH(OH)-CF_2-CF_2Br + O_2	→	O=CH-CF_2-CF_2Br + HO_2
	Then	
O=CH-CF_2-CF_2Br + OH	→	C(O)-CF_2-CF_2Br + H_2O
C(O)-CF_2-CF_2Br + O_2 (+ M)	→	C(O)O_2-CF_2-CF_2Br (+ M)
C(O)O_2-CF_2-CF_2Br + NO	→	C(O)O-CF_2-CF_2Br + NO_2
C(O)O-CF_2-CF_2Br	→	CO_2 + CF_2-CF_2Br
CF_2-CF_2Br + O_2	→	$BrCF_2$-CF_2O_2
$BrCF_2$-CF_2O_2 + NO	→	$BrCF_2$-CF_2O + NO_2
$BrCF_2$-CF_2O	→	$BrCF_2$ + CF_2O
$BrCF_2$ + O_2	→	$BrCF_2O_2$
$BrCF_2O_2$ + NO	→	$BrCF_2O$ + NO_2
$BrCF_2O$	→	CF_2O + Br

References

[1] Orkin, V. L.; Huie, R. E.; Kurylo, M. J. *J. Phys. Chem*. **1996**, *100*, 8907-8912.

[2] (a) Schlegel, H. B. *J. Chem. Phys.* **1986**, *84*, 4530. (b) Schlegel, H. B. *J. Phys. Chem.* **1988**, *92*, 3075 (c) Sosa, C.; Schlegel, H. B. *Int. J. Quantum Chem.* **1986**, *29*, 1001. (d) Sosa, C.; Schlegel, H. B. *Int. J. Quantum Chem.* **1987**, *30*, 155.

[3] (a) Johnston, H. S. *Gas Phase Reaction Rate Theory*; The Roland Press Company: New York, 1966. (b) Laidler, K.J. *Theories of Chemical Reaction Rates*, McGraw-Hill: New York, 1969. (c) Weston, R.E.; Schwartz, H.A. *Chemical Kinetics*, Prentice-Hall: New York, 1972. (d) Rapp, D. *Statistical Mechanics*, Holt, Reinhard, and Winston: New York, 1972. (e) Nikitin, E.E. *Theory of Elementary Atomic and Molecular Processes in Gases*, Claredon Press: Oxford, 1974. (f) Smith, I.W.M. *Kinetics and Dynamics of Elementary Gas Reactions*, Butterworths: London, 1980. (g) Steinfeld, J.I.; Francisco, J.S.; Hase, W.L. *Chemical Kinetics and Dynamics*, Prentice-Hall: New Jersey, 1989.

[4] Wigner, E.P. *Z.Phys.Chem.* **1932**, *B19*, 203.

[5] Rate constants calculated with the Turbo-Rate module in the beta version of the TURBO-OPT geometry optimization package, developed by C. Gonzalez and Tom Allison, National Institute of Standards and Technology, Gaithersburg, MD.

[6] *Scientific Assessment of Ozone Depletion: 1998*, Global Ozone Research and Monitoring Project, Report No. 44; World Meteorological Organization: Geneva, Switzerland, 1999.

[7] (a) Louis, F.; Gonzalez, C.A.; Huie, R. E.; Kurylo, M. J. *J. Phys. Chem. A* **2000**, *104*, 2931. (b) Louis, F.; Gonzalez, C.A.; Huie, R. E.; Kurylo, M. J. *J. Phys. Chem. A* **2000**, *104*, 8773.

[8] Louis, F.; Gonzalez, C.A.; Huie, R. E.; Kurylo, M. J. *J. Phys. Chem. A* **2001**, *105*. 1599.